

Downlink WCDMA Receivers Based on Combined Chip and Symbol Level Equalization

Ahmet Baştuğ

Philips Semiconductors, 06560, Sophia Antipolis, FRANCE

tel: +33 4 9294 4130, fax: +33 4 9296 1280, e-mail: ahmet.bastug@philips.com

Dirk T.M. Slock

Eurecom Institute, 06904, Sophia Antipolis, FRANCE

tel: +33 4 9300 2606 fax: +33 4 9300 2627, e-mail: slock@eurecom.fr

Abstract

In this paper we consider iterative receiver techniques for the downlink in WCDMA systems (UMTS FDD mode). We start from the linear MMSE receiver (at symbol level), which is time-varying and hence too complex to implement. By applying polynomial expansion (PE) to the LMMSE receiver, an iterative solution is obtained in which the complexity per iteration becomes comparable to twice that of the RAKE receiver. Our one contribution is to replace the channel matched filter by a channel equalizer within this PE to accelerate the convergence of the iterations. We also investigate various scenarios for the introduction of nonlinearities in the PE scheme that are particularly applicable to the multicode case of the High Speed Downlink Packet Access (HSDPA) mode since it is well known that nonlinearities in the PE scheme lead in fact to the Parallel Interference Canceller (PIC).

I. INTRODUCTION

Orthogonal variable spreading factor (OVSF) codes are used in most of the direct sequence code division multiple access (DS-CDMA) systems where multi-rate is considered for providing various levels of quality of service (QoS). The Universal Mobile Telecommunications System, Frequency Division Duplexed (UMTS-FDD) downlink is a particular example where user symbols are spread by factors ranging from 4 to 512. In this and in other similar systems, although the transmitted user signals at the base station (BS) side are orthogonal, this orthogonality no longer exists at the mobile station (MS) front-end due to the multipath effect of the propagation channel between the transmitter and the receiver.

There are three common approaches to circumvent this problem. The most straightforward and basic approach is to treat the generated interference due to multipath as an additive white gaussian noise (AWGN) and refer to the conventional *SNR-maximizing* Rake receiver to detect symbols of a code independently from others by collecting the energy via correlations with that code from the delayed forms of the received signal at multipath instants [1]. This approach is very much suboptimal since the inherent multiuser interference is far from being white containing some *predictable* portions. The second approach is the *interference suppression* where orthogonality is totally or partially brought back via the usage of chip level *SIR-maximizing* zero-forcing (ZF) or *SINR-maximizing* minimum mean square error (MMSE) channel equalizers and again the symbol estimates of a code are obtained independently from other codes via correlating the equalized chip sequence with that particular code [2], [3], [4], [5]. The third group of methods are *multiuser detectors* (MUD) which apply linear or nonlinear transformations to, in most cases, the output symbol estimates of Rake receivers (sparsified channel matched filter correlator cascade) of all codes [6], [7]. The two well known state-of-the-art linear MUDs are the decorrelating receiver and the LMMSE receiver [8], [9]. Unfortunately, they require inversions of large user cross-correlation matrices and hence they are not much practical. Other suboptimal MUDs that *explicitly* focus on subtracting the signals of interfering codes are called *interference cancellers* (IC). In parallel interference cancellation (PIC), Rake receiver output symbol estimates of each spreading code are progressively improved in a number of stages by *in parallel* deciding for and respreading also the symbols of all the other known codes, rechanneling their obtained chip sequences and subtracting their resultant signals from the originally received signal [10]. In serial interference cancellation (SIC), however, the purification of the received signal is done by cancelling the contributions of codes *one by one* starting with the code having the highest power [11]. SIC is expected to perform better when there is a nonnegligible variance among the user powers. However it is less popular due to the necessity of user ordering and due to the long incurred delay. Hence, PIC is more preferable although it requires more hardware.

It is well known that when the number of iterations goes to infinity, PIC *might* converge to the decorrelating receiver under very relaxed cell loads. However, provided that it converges, still the convergence rate is very slow and it requires many stages to obtain a reasonable performance. This is due to the existence of high cross-correlations among users [12], which in fact is a consequence of the low *orthogality factors* that can be obtained initially from the usage of Rake receivers in the front-end [13], [14].

In this paper, in order to guarantee the convergence (at least within practical load settings) and increase its speed, we start the decorrelation operation (*symbol level* ZF equalization) from the outputs of channel

equalizer-correlator type front-end receivers whose orthogonality factors are higher than those of Rake receivers. For *approximating* the decorrelation (a matrix inversion operation), we consider the polynomial expansion technique [15].

MUD has been rarely considered for the downlink since it requires the knowledge of active codes and their powers. However a simple method was proposed to detect the existence of *effective codes* from the comparisons of the Unitary Fast Walsh Hadamard Transform (U-FWHT) output power estimates at *the highest active* spreading factor level with an optimized threshold [16]. These effective codes might be used in place of the *unknown actual codes* since the actual symbol estimates and their powers are not necessary as long as the pseudo-symbols are treated linearly in interference cancellation. However, knowing or detecting the actual codes is an opportunity for exploiting hard or hyperbolic-tangent nonlinearities (or even channel decoding and encoding) to refine their symbol estimates [17], [10].

Appropriately sized U-FWHTs can also be used to realize the two-way transformations between actual symbol sequences at various SF levels and their multiple pseudo-symbol sequence equivalents at the highest active SF level. In other words, multi-rate can be modelled as multicode and one can easily extract the actual symbols of the *known codes* at any level by applying an appropriate U-FWHT to the corresponding group of pseudo symbols. This is demonstrated in Fig. 1 where L_2/L_1 consecutive (time-multiplexed) a_i actual symbols at level L_1 are reflected to again L_2/L_1 parallel (code-multiplexed) \tilde{a}_i pseudo-symbols at level L_2 . $P_{\{L_2/L_1\}}/S$ and $S/P_{\{L_2/L_1\}}$ are parallel to serial and serial to parallel converters from/to a bus size L_2/L_1 . In most parts of this paper, we will exploit the *effectiveness* concept at the highest *active* SF-256 in the UMTS-FDD downlink for applying polynomial expansion at this level. We will ignore the existence of SF-512 since it is rarely used carrying control commands during an upload operation.

Without loss of generality, our main concern for the usage of the proposed ICs is the high speed packet data access (HSDPA) service standardized in Release-5 [18], [19]. In HSDPA, one or more of the High Speed Downlink Shared Channels (HSDSCHs) at SF-16, in particular 1,5,10 or 15 of the 16 available codes, are time multiplexed (scheduled) among users, preferably all allocated to a single user at any time. The goal is to exploit *multiuser diversity*, i.e the temporal channel quality variance among the users, in order to increase the *sum capacity*, that is the total delivered payload by the BS. It is up to the operators to choose the types of schedulers compromising throughput and fairness depending on the predicted channel quality, the cell load and the traffic priority class. A better performing mobile receiver is quite beneficial in HSDPA services since unlike for dedicated channels (DCHs) where it serves only for the benefit of the base station, for HSDSCHs, a mobile terminal directly benefits from having an

advanced receiver by obtaining more data rate once the connection is established and by increasing the chance of getting a connection if fairness is partially sacrificed for capacity in user scheduling. What is important here for the design of advanced receivers is the added knowledge of the identities of possibly more than one equally powered codes. We will benefit from this side information to refine the globally linearly formulated polynomial expansion receivers via replacing some local receiver ingredients with their nonlinear equivalents. We will also exploit the knowledge of the pilot tone to decrease its level of interference by efficiently hard-subtracting it [20].

The paper is organized as follows: In Section II, we give the transmission model in the UMTS FDD downlink and elaborate on the stationarity of the sampled received signal. In Section III, we derive iterative receiver expressions via the polynomial expansion technique. In Section IV, we cover the receivers at first order and the local MMSE improvements over their certain ingredients. In Section V, we look at multiple orders and discuss many receiver variants. Section VI and Section VII are devoted to simulations and conclusions.

II. BASEBAND DOWNLINK TRANSMISSION MODEL

The baseband downlink transmission model of a CDMA-based cellular system with an interfering neighboring cell, BS_2 , is demonstrated in Fig. 2. In practice, however, this model on which we base our discussion can be generalized to multiple interfering base stations. For each base station BS_j , s.t. $j \in \{1, 2\}$, the K_j (pseudo-)user signals are transmitted over the same linear multipath channel $h_j(t)$ since we assume that downlink user signals are chip-synchronous and there is no beamforming. The symbol and chip periods T and T_c are related through the spreading factor L as $T=L \times T_c$, which here is assumed to be common for all the (pseudo-)users and for the two base stations. As explained before, in a multi-rate system where the receiver operates at the highest active SF level L , we might model each users' code of spreading factor, $\mathcal{L}_{j,k}$, as being equivalent to a combinations (via conceptual U-FWHT) of $L/\mathcal{L}_{j,k}$ orthogonal codes with length L . The total chip sequences $b_j[l]$ are the sums of the chip sequences of all the (pseudo-)users for BS_j . Every (pseudo-)user chip sequence $b_{j,k}[l]$ is given by the convolution of the L times upsampled form, $a_{j,k}^L[l]$, of the (pseudo-)symbol sequence $a_{j,k}[n]$ (s.t. $n = \lfloor \frac{l}{L} \rfloor$) and an aperiodic spreading sequence $w_{j,k}[l]$ which is itself in UMTS FDD, the product of a periodic, unit energy Walsh-Hadamard spreading sequence $c_{j,k}[l \bmod L]$, and a base-station specific unit magnitude complex scrambling sequence $s_j[l]$ as $w_{j,k}[l] = c_{j,k}[l \bmod L]s_j[l]$:

$$b_j[l] = \sum_{k=1}^{K_j} b_{j,k}[l] = \sum_{k=1}^{K_j} \sum_{i=-\infty}^{\infty} a_{j,k}^L[i]w_{j,k}[l-i] \quad j \in \{1, 2\} \quad (1)$$

The chip sequences $b_1[l]$ and $b_2[l]$ pass through similar pulse shape filters $p(t)$, their corresponding propagation channels $h_1(t)$ and $h_2(t)$ and the antialiasing filter at the receiver front end before getting sampled. After sampling, these two overall continuous time transmission channels can be interpreted as discrete multi-channels by the mobile receiver if the signal is captured by q sensors and/or sampled at an integer multiple m of the chip rate, rendering the total number of samples per chip $m q > 1$. Stacking these $m q$ samples in vectors representing samples in one chip period, we get the sampled received vector signal

$$\begin{aligned} \mathbf{y}[l] &= \mathbf{y}_1[l] + \mathbf{y}_2[l] + \mathbf{v}[l] \\ \mathbf{y}_j[l] &= \sum_{k=1}^{K_j} \sum_{i=0}^{N-1} \mathbf{h}_j[i] b_{j,k}[l-i] \quad j \in \{1, 2\} \end{aligned} \quad (2)$$

where

$$\begin{aligned} \mathbf{y}_j[l] &= \left[y_{j,1}[l] \dots y_{j,mq}[l] \right]^T, \\ \mathbf{h}_j[l] &= \left[h_{j,1}[l] \dots h_{j,mq}[l] \right]^T, \\ \mathbf{v}[l] &= \left[v_1[l] \dots v_{mq}[l] \right]^T. \end{aligned} \quad (3)$$

Here, with a slight abuse of notation, $\mathbf{h}_j[l]$ represents the vectorized samples (represented at chip rate) of the overall channels (assumed to have the same delay spread of N chips) including the pulse shape, the propagation channel and the antialiasing receiver filter.

When we model the scramblers as unknown, i.i.d, aperiodic sequences and the symbol sequences as i.i.d., stationary, white sequences, then the chip sequences $b_{\{1,2\}}[l]$ are also stationary and white. Therefore, both the intracell and intercell contribution to $\mathbf{y}[l]$ are vector stationary processes the continuous-time counterparts of which are cyclostationary with chip period. Finally, the remaining noise, $\mathbf{v}[l]$, also assumed to be white and stationary, the sum of interference and noise represented at chip rate is vector stationary.

III. SYMBOL LEVEL EQUALIZATION BY POLYNOMIAL EXPANSION

In this section, we develop intra and intercell interference cancelling (IC) structures based on polynomial expansion (PE) technique which was initially proposed in [15].

Assuming without loss of generality that there is a single highly interfering BS, i.e. BS_2 , a vector of received signal over one symbol period can be written as

$$\begin{aligned} \mathbf{Y}[n] &= [\mathbf{H}_1(z) \mathbf{S}_1[n] \mathbf{C}_1 \quad \mathbf{H}_2(z) \mathbf{S}_2[n] \mathbf{C}_2] \begin{bmatrix} \mathbf{A}_1[n] \\ \mathbf{A}_2[n] \end{bmatrix} + \mathbf{V}[n] \\ &= \tilde{\mathbf{G}}(n, z) \mathbf{A}[n] + \mathbf{V}[n] \end{aligned} \quad (4)$$

representing the system at the symbol rate.

As shown in Fig. 3, $\mathbf{H}_j(z) = \sum_{i=0}^{M_j-1} \mathbf{H}_j[i] z^{-i}$ is the symbol rate $Lmq \times L$ channel transfer function, z^{-1} being the symbol period delay operator. The block coefficients $\mathbf{H}_j[i]$ are the $M_j = \lceil \frac{L+N_j+d_j-1}{L} \rceil$ parts of the block Toeplitz matrix with $mq \times 1$ sized blocks, \mathbf{h}_j being the first column whose top entries might be zero for it comprises the transmission delay d_j between BS_j and the mobile terminal. In this representation, $\mathbf{H}_j(0)$ carries the signal part corresponding to $\mathbf{A}_j[n]$ where there is no intersymbol interference (ISI) or multiuser intersymbol interference (MU-ISI) but only interchip interference (ICI) and multiuser interchip interference (MU-ICI). $\mathbf{H}_j(i)$, ($i \in \{1, 2, \dots, M_j - 1\}$), however, carries the ISI and MU-ISI from $\mathbf{A}_j[n - i]$. The $L \times L$ matrices $\mathbf{S}_j[n]$ are diagonal and contain the scrambler of BS_j for symbol period n . The column vectors $\mathbf{A}_j[n]$ contain the K_j (pseudo-)symbols of BS_j , $\mathbf{A}[n]$ contains the total $K = K_1 + K_2$ (pseudo-)user (pseudo-)symbols in two base stations, and \mathbf{C}_j is the $L \times K_j$ matrix of the K_j active codes for BS_j . Based on the equivalency of the chip rate and the symbol rate representations as demonstrated in Fig. 4 which shows the conversion between the two representations via serial-to-parallel and parallel-to-serial converters by vectorizing and sample rate conversion by a factor L , one can pass from the chip level models represented by (1), (2) and (3) to the symbol level model represented by (4) where $\tilde{\mathbf{G}}(n, z)$ is a $Lmq \times K$ channel-plus-spreading symbol rate filter. Although it is possible to find an FIR left inverse filter for $\tilde{\mathbf{G}}(n, z)$ provided that $Lmq \geq K$, this is not practical since $\tilde{\mathbf{G}}(n, z)$ is time-varying due to the aperiodicity of the scrambling. Therefore, we will introduce a less complex approximation to this inversion based on the polynomial expansion technique [15]. Instead of basing the receiver directly on the received signal, we shall first introduce a dimensionality reduction step (from Lmq to K) by equalizing the channels with minimum mean square error zero forcing (MMSE-ZF) chip rate equalizers $\mathbf{F}_j(z)$ followed by a bank of correlators. MMSE-ZF equalizer is the one among all possible ZF equalizers which minimizes the MSE at the output [21]. Let $\mathbf{X}[n]$ be the $K \times 1$ correlator output, which would correspond to the Rake receiver outputs if channel matched filters were used instead of channel equalizers. Then,

$$\begin{aligned} \mathbf{X}[n] &= \tilde{\mathbf{F}}(n, z) \mathbf{Y}[n] \\ &= \begin{bmatrix} \mathbf{C}_1^H \mathbf{S}_1^H[n] \mathbf{F}_1(z) \\ \mathbf{C}_2^H \mathbf{S}_2^H[n] \mathbf{F}_2(z) \end{bmatrix} (\tilde{\mathbf{G}}(n, z) \mathbf{A}[n] + \mathbf{V}[n]) \\ &= \mathbf{M}(n, z) \mathbf{A}[n] + \tilde{\mathbf{F}}(n, z) \mathbf{V}[n] \end{aligned}$$

where $\mathbf{M}(n, z) = \tilde{\mathbf{F}}(n, z)\tilde{\mathbf{G}}(n, z)$ and ZF equalization results in $\mathbf{F}_j(z)\mathbf{H}_j(z) = \mathbf{I}$. Hence,

$$\mathbf{M}(n, z) = \sum_{i=-\infty}^{\infty} \mathbf{M}[n, i]z^{-i} = \begin{bmatrix} \mathbf{I} & * \\ * & \mathbf{I} \end{bmatrix}$$

due to proper normalization of the code energies.

In order to obtain the estimate of $\mathbf{A}[n]$, we initially consider the processing of $\mathbf{X}[n]$ by a decorrelator as

$$\begin{aligned} \hat{\mathbf{A}}[n] &= \mathbf{M}(n, z)^{-1} \mathbf{X}[n] \\ &= (\mathbf{I} + \overline{\mathbf{M}}(n, z))^{-1} \mathbf{X}[n]. \end{aligned} \quad (5)$$

The correlation matrix $\mathbf{M}(n, z)$ has a coefficient $\mathbf{M}[n, 0]$ with a dominant unit diagonal in the sense that all other elements of the $\mathbf{M}[n, i]$ are much smaller than one in magnitude. Hence, the polynomial expansion approach suggests to develop $(\mathbf{I} + \overline{\mathbf{M}}(n, z))^{-1} = \sum_{i=0}^{\infty} (-\overline{\mathbf{M}}(n, z))^i$ up to some finite order, which after dropping indices leads to

$$\begin{aligned} \hat{\mathbf{A}}^{(-1)} &= 0 ; \quad i \geq 0 . \\ \hat{\mathbf{A}}^{(i)} &= \mathbf{X} - \overline{\mathbf{M}} \hat{\mathbf{A}}^{(i-1)} , \\ &= \mathbf{X} - (\mathbf{M} - \mathbf{I}) \hat{\mathbf{A}}^{(i-1)} , \\ &= \hat{\mathbf{A}}^{(i-1)} + \tilde{\mathbf{F}}^i (\mathbf{Y} - \tilde{\mathbf{G}}^i \hat{\mathbf{A}}^{(i-1)}) . \end{aligned} \quad (6)$$

Many receiver variants can be obtained starting from this derived expression. Practical constraints, however, limit the expansion to a few orders.

IV. SINGLE STAGE INTERFERENCE CANCELLATION

In this section we will discuss receiver architectures limited to first order polynomial expansion.

At first order, the expression for the user of interest (user one) becomes:

$$\begin{aligned} \hat{\mathbf{a}}_{1,1}^{(1)}[n] &= \mathbf{e}_1^H \hat{\mathbf{A}}^{(1)}[n] \\ &= \mathbf{e}_1^H (\mathbf{X}[n] - \overline{\mathbf{M}}(n, z) \hat{\mathbf{A}}^{(0)}[n]) \\ &= \mathbf{e}_1^H (2\mathbf{X}[n] - \mathbf{M}(n, z) \mathbf{X}[n]) \\ &= \mathbf{e}_1^H \tilde{\mathbf{F}}(n, z) (2\mathbf{Y}[n] - \tilde{\mathbf{G}}(n, z) \mathbf{X}[n]) \\ &= \mathbf{c}_{1,1}^H \mathbf{S}_1^H [n] \mathbf{F}_1(z) (2\mathbf{Y}[n] - \tilde{\mathbf{G}}(n, z) \tilde{\mathbf{F}}(n, z) \mathbf{Y}[n]) \end{aligned} \quad (7)$$

where \mathbf{e}_i ($i \in \{1, 2, \dots, K\}$) is a column vector having a 1 at the i^{th} position and the rest filled with 0s. From this symbol rate equation, one can obtain the chip rate signal processing diagram in Fig. 5 by using

the equivalencies in Fig. 4. Each branch in the IC block is formed in order by a linear filter ($\{\mathbf{f}_1, \mathbf{f}_2\}$), a downsampler, a descrambler, a serial to parallel converter, a despreader, a resreader $\{\mathbf{g}_1, \mathbf{g}_2\}$, a parallel to serial converter, a scrambler, an upsampler and a re-channeling filter.

Now that we have obtained the first order *polynomial expansion decorrelating structure*, we look for an *equivalent interference cancelling representation* that excludes the user signal estimation operation in the first IC branch. Let

$$\begin{aligned}\mathbf{I}_{K \times K} &= [\mathbf{e}_1 \mathbf{e}_2 \dots \mathbf{e}_K] = [\mathbf{e}_1 \bar{\mathbf{e}}_1] \\ \tilde{\mathbf{G}}(n, z) &= [\tilde{\mathbf{g}}_1(n, z) \bar{\mathbf{G}}_1(n, z)] \\ \tilde{\mathbf{F}}(n, z) &= [\tilde{\mathbf{f}}_1(n, z)^T \bar{\mathbf{F}}_1(n, z)^T]^T \\ \mathbf{A}[n] &= [a_{1,1}[n] \bar{\mathbf{A}}_1[n]^T]^T \\ \tilde{\mathbf{f}}_1(n, z) \tilde{\mathbf{g}}_1(n, z) &= 1.\end{aligned}$$

Then, dropping the indices and starting from (7), we obtain

$$\begin{aligned}\hat{\mathbf{a}}_{1,1}^{(1)} &= (2\tilde{\mathbf{f}}_1 \tilde{\mathbf{g}}_1 - \tilde{\mathbf{f}}_1 \tilde{\mathbf{g}}_1 \tilde{\mathbf{f}}_1 \tilde{\mathbf{g}}_1 - \tilde{\mathbf{f}}_1 \bar{\mathbf{G}}_1 \bar{\mathbf{F}}_1 \tilde{\mathbf{g}}_1) \mathbf{a}_{1,1} + (2\tilde{\mathbf{f}}_1 \bar{\mathbf{G}}_1 - \tilde{\mathbf{f}}_1 \tilde{\mathbf{g}}_1 \tilde{\mathbf{f}}_1 \bar{\mathbf{G}}_1 - \tilde{\mathbf{f}}_1 \bar{\mathbf{G}}_1 \bar{\mathbf{F}}_1 \bar{\mathbf{G}}_1) \bar{\mathbf{A}}_1 \\ &= (\tilde{\mathbf{f}}_1 \tilde{\mathbf{g}}_1 - \tilde{\mathbf{f}}_1 \bar{\mathbf{G}}_1 \bar{\mathbf{F}}_1 \tilde{\mathbf{g}}_1) \mathbf{a}_{1,1} + (\tilde{\mathbf{f}}_1 \bar{\mathbf{G}}_1 - \tilde{\mathbf{f}}_1 \bar{\mathbf{G}}_1 \bar{\mathbf{F}}_1 \bar{\mathbf{G}}_1) \bar{\mathbf{A}}_1 \\ &= \tilde{\mathbf{f}}_1 (\mathbf{I} - \bar{\mathbf{G}}_1 \bar{\mathbf{F}}_1) \mathbf{Y} \\ &= \mathbf{e}_1^H \tilde{\mathbf{F}} (\mathbf{Y} - \tilde{\mathbf{G}} \bar{\mathbf{e}}_1 \bar{\mathbf{e}}_1^H \tilde{\mathbf{F}} \mathbf{Y}) \\ &= \mathbf{e}_1^H \tilde{\mathbf{F}} (\mathbf{Y} - \bar{\mathbf{G}}_1 \bar{\mathbf{F}}_1 \mathbf{Y}).\end{aligned}$$

This first order estimation process has now the form of an interference canceller as shown in Fig. 6. Different from the polynomial expansion structure, there is here no multiplicative factor of two at the top line and $\bar{\mathbf{C}}_1, \bar{\mathbf{C}}_1^H$ correspond to (de)spreading with the intracell interferer's codes, namely excluding the user code. So, the top IC branch handles intracell interference whereas the bottom IC branch handles intercell interference. We also made some changes like introducing nonlinear processors $\zeta(\cdot)$ in between the despreader and the spreader modules and replacing \mathbf{f}_1 after the subtractor by \mathbf{f}_3 the purposes of which will be explained next.

A. Local MMMSE Operations

One of the advantages of the MMSE-ZF approach w.r.t. the MMSE approach is that clear symbol and chip sequence estimates appear at various points in the receiver which can be improved locally by replacing whatever the global MMSE-ZF structure yields as estimates by improved estimates in the MMSE

sense. Any local MMSE improvement should lead to global MMSE improvement. In an iterative PE approach, such modifications should also lead to smaller offdiagonal power and hence faster convergence of the iterations to an estimate that is closer to a MMSE estimate. The interpretations to be discussed though being applicative to any iteration with the possible dependance of a number of quantities on the iteration index, in this section we will concentrate only on the first iteration displayed in Fig. 6 where the role of filters \mathbf{f}_1 and \mathbf{f}_2 is to produce the estimates of the chip sequences of BS_1 and BS_2 . Those estimates can be improved by replacing the considered so far MMSE-ZF chip rate equalizers \mathbf{f}_1 and \mathbf{f}_2 by MMSE equalizers which, though perturb the orthogonal structure of the received signal from the BS, do not enhance as much the intercell interference plus noise [22]. The estimated chip sequence then gets descrambled and passes by correlators to produce symbol estimates for the intracell/intercell interferers. These symbol estimates can be improved in a variety of ways by symbolwise linear or nonlinear functions $\zeta(\cdot)$ like exploiting the symbol variance to introduce an LMMSE weighting factor or exploiting the symbol constellation by taking *hard decisions* which however possibly does not improve the estimate. Hence, one may replace the hard decision by a variety of *soft decisions*. A locally optimal MMSE estimate is obtained by using a *hyperbolic tangent* function and the estimated symbols are then respread, scrambled and added to produce again an estimate of the chip sequence. The purpose of the rechanneling filters \mathbf{g}_j (so far equivalent to the channel impulse response \mathbf{h}_j) is to produce an intracell/intercell interference estimate at the level of the received signal, on the basis of the chip sequences estimates. The linear filter after the IC canceller \mathbf{f}_3 which is considered to be equal to \mathbf{f}_1 in the polynomial expansion setup can also be (in fact *must* be in case of local MMSE modifications on the IC branches) replaced by a Rake or an LMMSE filter. The second one would perform better but it requires the estimation of structured residual interferences from the two base stations.

As explained before, for the spreading and despreading with the Walsh-Hadamard codes of the active users, it is suggested to (de)spread with all WH codes simultaneously, which can be done with the Fast Walsh-Hadamard transform (FWHT) [16]. The detection of used vs. unused codes occurs implicitly when the powers associated with the codes get estimated at correlator outputs. With the assumption of the correct detections, correlator outputs corresponding to nonactive codes are excluded.

The multirate case corresponding to variable spreading factors can be reformulated as a multicode case. The tree structure of the orthogonal variable spreading factors (OVSFs) allows to interpret the interfering users as equivalent low rate pseudo-users at least when the symbol constellation of the interferers will not get exploited, in which case only secondorder statistics count. Hence, in that case one needs at most

to consider the multicode equivalency at a lower rate for the user of interest. If on the other hand one also desires to exploit the interferers' symbol constellation, then one needs to detect and use the actual spreading factors of the interferers. The tree structure of the OVSFs can be exploited to progressively explore increasing spreading factors and investigate the finite alphabet hypothesis at the various tree branches. In this case one cannot use the FWHT as such but the ingredients leading to its derivation (OVSF in fact) can still be used for fast (de)spreading.

The implementations of the hyperbolic tangent and the hard decisions requires the estimation of the user symbol powers. Let $\mathbf{z}_{i,j}$ represent the chip-rate channel-MMSE filter cascade of \mathbf{h}_j and \mathbf{f}_i including the external (up/down) samplers. Then, the expected value of the received power after the k^{th} decorrelator on the first branch is equal to

$$\begin{aligned}\beta_{1,k} &= |z_{1,1}(0)|^2 |a_{1,k}|^2 + \frac{1}{L} (\|\mathbf{z}_{1,1}\|^2 - |z_{1,1}(0)|^2) \sum_{i=1}^{K_1} |a_{1,i}|^2 + \frac{1}{L} \|\mathbf{z}_{1,2}\|^2 \sum_{i=1}^{K_2} |a_{2,i}|^2 + \sigma_v^2 \|f_1\|^2 \\ &= |z_{1,1}(0)|^2 |a_{1,k}|^2 + (\|\mathbf{z}_{1,1}\|^2 - |z_{1,1}(0)|^2) \sigma_1^2 + \|\mathbf{z}_{1,2}\|^2 \sigma_2^2 + \sigma_v^2 \|f_1\|^2 \\ &= |z_{1,1}(0)|^2 |a_{1,k}|^2 + \sigma_{n1}^2\end{aligned}$$

since the expected value of the correlation coefficient between any two nonorthogonal codes or between two shifted versions of the same code is equal to $1/L$; zero-forced channel coefficient is $z_{1,1}(0)$ (which is in fact equal to 1 for the unbiased MMSE case) and $\|f_1\| = 1$. We assume that we know the channel parameters, the total received power from both base stations and the noise variance but we do not know each single user's power. Therefore, the estimate of $|a_{1,k}|^2$, i.e. $|\alpha_{1,k}|^2$, can be calculated by subtracting the effective interference σ_{n1}^2 from the long term average power $\beta_{1,k}$ and scaling by $1/|z_{1,1}(0)|^2$. If the result is negative we replace it by 0. The powers of users in the second cell are estimated similarly.

For the MMSE filter construction after the subtractor, estimation of total leakage interference powers originating from the two base stations are necessary. Let γ_{1int} , γ_{2int} and σ_{user1}^2 be the average chip rate measured powers before the rescrambler blocks in the two IC branches and the user chip rate power respectively. Then, $\sigma_{leak1}^2 = |\sigma_1^2 - \sigma_{user1}^2 - \gamma_{1int}|$ and $\sigma_{leak2}^2 = |\sigma_2^2 - \gamma_{2int}|$.

In the sequel, for simulations we will consider the symbols from QPSK constellation. Hence, we give here the optimal tangent hyperbolic estimator and the hard estimator for received QPSK symbols

$$r_{j,k} = \chi_{j,k} + i \psi_{j,k}:$$

$$\begin{aligned}\hat{\mathbf{a}}_{j,k}^{thyp} &= \frac{\alpha_{j,k}}{\sqrt{2}} \tanh(\sqrt{2} |z_{1,1}(0)| \frac{\alpha_{j,k}}{\sigma_{nj}^2} \chi_{j,k}) + i \frac{\alpha_{j,k}}{\sqrt{2}} \tanh(\sqrt{2} |z_{1,1}(0)| \frac{\alpha_{j,k}}{\sigma_{nj}^2} \psi_{j,k}) \\ \hat{\mathbf{a}}_{j,k}^{hard} &= \frac{\alpha_{j,k}}{\sqrt{2}} (\text{sign}(\chi) + i \text{sign}(\psi))\end{aligned}$$

The corresponding nonlinear curves are demonstrated in Fig. 9 together with 45 degree sloped linear decision line.

B. Simulations at a Unique Spreading Factor

For the simulations specific to this section we will consider a single-rate (unique spreading factor) transmission system. The K_j users of base station j are considered synchronous between them, with the same spreading factor 32 and using the same downlink channel \mathbf{h}_j , an FIR filter which is the result of the convolution of a sparse Vehicular A UMTS channel and a root-raised cosine pulse shape with roll-off factor of 0.22. The channel length is $N = 19$ chips due to the UMTS chip rate of 3.84 Mchips/sec. An oversampling factor of $m = 2$ and one receive antenna $q = 1$ are used. User symbols are from QPSK constellation. The user of interest has 10dB less power than an average single interferer power which represents the *near-far situation*. Fig. 7 and Fig. 8 show the SINR performance of the proposed receivers and the classical reference Rake receiver (channel matched filter and correlator cascade). As expected, they outperform the Rake receiver with high margins. Hard estimation and hyperbolic estimations give better results than the projector, hyperbolic decision performing slightly better. As for the linear filter after the subtractor, the LMMSE equalizer which is constructed based on the residual interference powers from the two IC branches outperforms the Rake receiver.

V. MULTI-STAGE INTERFERENCE CANCELLATION

A practical receiver would be limited to a few orders, the quality of which depends on the degree of dominance of the static part of the diagonal of $\mathbf{M}(n, z)$ given in (6) with respect to its multiuser interference (MUI) carrying off-diagonal elements and the ISI carrying dynamic contents of the diagonal elements. In order to increase the degree of this dominance, we revise (6) by introducing symbol feedback nonlinearities which leads us to the multistage receiver architecture in Fig. 10. There, we also demonstrate the option of hard subtracting the pilot tone contribution $\tilde{\mathbf{G}}^P \mathbf{A}^P$. After these revisions, the initial formulations should be expanded as:

$$\begin{aligned} \tilde{\mathbf{G}} \mathbf{A} &= \begin{bmatrix} \tilde{\mathbf{G}}^P & \tilde{\mathbf{G}}^D \end{bmatrix} \begin{bmatrix} \mathbf{A}^P \\ \mathbf{A}^D \end{bmatrix} \\ \mathbf{Y}^D &= \mathbf{Y} - \tilde{\mathbf{G}}^P \mathbf{A}^P \\ \hat{\mathbf{A}}^{D(i)} &= \hat{\mathbf{A}}^{D(i-1)} + \tilde{\mathbf{F}}^{D(i)} (\mathbf{Y}^D - \tilde{\mathbf{G}}^{D(i)} \hat{\mathbf{A}}^{D(i-1)}) \\ \hat{\tilde{\mathbf{A}}}^{D(i)} &= \zeta^{D(i)} (\hat{\mathbf{A}}^{D(i)}) \end{aligned}$$

The superscripts P and D correspond to the pilot-tone and the data parts respectively. In Fig. 10, the numbers in parantheses indicate the iterations where the local functionalities reside. One thing to note down at this point which is valid for also the receivers to be explained later is that local functionalities such as equalizers, rechanneling filters and nonlinear symbol estimators might be optimized according to iteration-dependant residual signal power levels.

For the moment, we consider LMMSE chip rate equalizers and exact channel filters within the $\tilde{\mathbf{F}}$ and $\tilde{\mathbf{G}}$ symbol rate filters. In practice, LMMSE equalizer should be implemented as a generalized Rake (G-Rake) receiver [23]. In that case, in every interference estimator and canceller (IEC) block shown in Fig. 11, filtering with $\tilde{\mathbf{F}}$ and $\tilde{\mathbf{G}}$ will have the same complexity of a Rake receiver. Hence, the filtering parts of each iteration will have twice the complexity of those of Rake. It is also of interest to compare the performance of such a scheme with another more adopted one (e.g conventional PIC) where channel matched filters are used instead of equalizers. When channel matched filters are used, then it is clear that due to obtained low orthogonality factors there will be a convergence problem if exact channel filters are considered for $\tilde{\mathbf{G}}$. In that case Wiener filters should be considered as, vaguely saying, rechanneling filters to minimize the mean square error after the subtractors. Weighted forms of hard symbol decisions might also accompany the Wiener filters to achieve this.

In the straight linear PE case, the ζ symbol estimator block is the identity matrix everywhere. Those diagonal parts corresponding to the known actual codes, however, can be replaced by symbol feedback functionalities like hard-decisions, hyperbolic tangent nonlinearities or even channel decoding and encoding blocks to increase the dominancy of the static contents of the diagonal part of the iteration dependant user cross correlation matrix. The input and the output estimates of such blocks are represented by $\hat{\mathbf{A}}$ and $\hat{\hat{\mathbf{A}}}$ respectively. To adopt such an hybrid approach, one can utilize appropriately sized FWHTs (or multiple correlators depending on the gain or loss) as shown in Fig. 1 to move back and forth between the actual symbols of the known codes and their pseudo-symbol equivalents at PE level. The proper way of applying the hyperbolic tangent nonlinearities is to reestimate the bending parameter (i.e the interference + noise variance) in every iteration. It is simply the difference between the actual symbol power and the moving average estimate of the received symbol powers.

Many other variants of the proposed receiver can be derived. A reasonable approach would be to sepearate the data part into two categories D_1 and D_2 which correspond to multiple HSDSCH codes (i.e codes with known power) and the rest (i.e codes whose power are unknown but above a threshold set at FWHT outputs) respectively. One might then treat the symbols of D_1 by estimating and cancelling them

via exploiting nonlinearities and treat the symbols of D_2 linearly by PE.

Putting the code of interest in one or the other category leads to two different receiver families which might both be explained over Fig. 12. When we put it in D_2 , then the corresponding set of equations will be

$$\begin{aligned}\tilde{\mathbf{G}} \mathbf{A} &= \begin{bmatrix} \tilde{\mathbf{G}}^P & \tilde{\mathbf{G}}^{D_1} & \tilde{\mathbf{G}}^{D_2} \end{bmatrix} \begin{bmatrix} \mathbf{A}^P \\ \mathbf{A}^{D_1} \\ \mathbf{A}^{D_2} \end{bmatrix} \\ \mathbf{Y}^{D_2} &= \mathbf{Y} - \tilde{\mathbf{G}}^P \mathbf{A}^P - \tilde{\mathbf{G}}^{D_1(1)} \hat{\mathbf{A}}^{D_1(0)} \\ \hat{\mathbf{A}}^{D_2(-1)} &= 0 \\ \hat{\mathbf{A}}^{D_2(i)} &= \hat{\mathbf{A}}^{D_2(i-1)} + \tilde{\mathbf{F}}^{D_2(i)} (\mathbf{Y}^{D_2} - \tilde{\mathbf{G}}^{D_2(i)} \hat{\mathbf{A}}^{D_2(i-1)}) \\ \hat{\mathbf{A}}^{D_2(i)} &= \zeta^{D_2(i)} (\hat{\mathbf{A}}^{D_2(i)})\end{aligned}$$

In this case, in an initial step we cancel the interference of HSDSCH codes and then similar to the setting explained in Fig. 10 we iterate on the code of interest with others for a number of PE stages. Hence, there is no need for the final dashed block in Fig. 12. When we put the code of interest in D_1 , however, the initial block cancels the estimated signals of all HSDSCH codes including the signal of interest. In the second block, PE expansion estimates all the remaining interference. Due to the absence of also signal of interest, here we expect a better estimation than the first scenario. Then, this estimate is deleted from the originally received signal and in the third block interference cancellation is applied among the HSDSCH codes. Although not shown on the figure, it is also possible to iterate many stages in the third block. The extra set of equations corresponding to the third block will then be

$$\begin{aligned}\mathbf{Y}^{D_1} &= \mathbf{Y} - \tilde{\mathbf{G}}^P \mathbf{A}^P - \tilde{\mathbf{G}}^{D_2(p)} \hat{\mathbf{A}}^{D_2(p-1)} \\ \hat{\mathbf{A}}^{D_1(-1)} &= 0 \\ \hat{\mathbf{A}}^{D_1(i)} &= \hat{\mathbf{A}}^{D_1(i-1)} + \tilde{\mathbf{F}}^{D_1(i)} (\mathbf{Y}^{D_1} - \tilde{\mathbf{G}}^{D_1(i)} \hat{\mathbf{A}}^{D_1(i-1)}) \\ \hat{\mathbf{A}}^{D_1(i)} &= \zeta^{D_1(i)} (\hat{\mathbf{A}}^{D_1(i)})\end{aligned}$$

The second approach is clearly more efficient in terms of the implementation cost when there are multicode of interest. Because, in that case the PE stages would be different for each code of interest when the first approach is adopted.

Such group partitioned receivers have a serious drawback. If the interference of the known codes is not cancelled very reliably in the first stage, then the leakage interference will result in dramatic deterioration of the performance during following PE stages. To remedy the situation, known codes can be contained in the PE as well. However the improvement w.r.t the straight PE over all known and unknown codes

will be very negligible. We believe that such a SIC-PIC-hybrid approach would work well when channel decoding and encoding is adopted as the symbol feedback functionality. This would decrease the leakage below a maximum tolerated value.

VI. SIMULATIONS

For the simulations, we take an HSDPA service scenario in the UMTS FDD downlink as follows: There are 5 HSDSCH codes at SF-16 each consuming 8% of the BS power. The pilot tone at SF-256 consumes 10% power. There is the PCCPCH code at SF-256 that consumes 4% power. To effectively model all the rest multirate user codes that we do not know, we place 46 pseudo-codes at level 256 each having 1% power. So in total, 5 HSDSCH codes at SF-16 being equivalent to 80 pseudo-codes at SF-256, the system is effectively 50% loaded. We assume that all the five HSDSCH codes belong to the user of interest; hence they are known. Other than those, we know the code (even the content) of the pilot tone. So we consider hard subtracting it. Although we know the PCCPCH code, we leave it within the group of unknown codes. We model an interfering second BS having the same properties with the only exception that we assume we do not know its HSDSCH codes and hence we treat them only linearly. Although, in practice, the effective codes should be detected by a method explained in the text, for the moment, we assume that they are known. We also assume perfect knowledge of channels. An oversampling factor of $m = 2$ and one receive antenna $q = 1$ are used. The propagation channels are randomly generated from the ITU Vehicular-A channel model. Pulse shape is the UMTS-standard, root-raised cosine with a roll-off factor of 0.22. Therefore the propagation channel, pulse shape cascade (i.e the overall channel) has a length of 19 chips at 3.84 Mchips/sec transmission rate. Symbols are QPSK symbols. Note that for HSDSCHs, 16-QAM is also a possibility but so far we did not consider it.

Fig. 13 shows the SINR versus input E_b/N_0 results corresponding to the receiver architecture in Fig. 10. Here we treat all the codes linearly (identity matrix as symbol feedback) and we do not subtract the pilot tone. We consider both LMMSE equalizer and channel matched filter for the chip rate filtering. As seen from the figure, there is a dramatic consequence of choosing one for another. The performance improves with every iteration when LMMSE equalizers are used whereas the trend is in the reverse direction for the channel matched filters. This result can be attributed to the difference between orthogonality factors at the two filter outputs. One can implicitly see this by observing the 0^{th} iteration outputs d_0 and c_0 where there is more than 6 dB gap between LMMSE-Equalizer and CMF performance. This result indicates that if the initial stage does not perform over a cell load dependant threshold, then the iterations will diverge.

Provided that divergence is avoided, still the speed of convergence highly depends on the used chip rate filter.

When we look at the performance of equalizers in Fig. 13, we see that the amount of improvement between iterations depend on the input E_b/N_0 (SNR in other words). Early iterations saturate also earlier as we move along increasing E_b/N_0 axis. The difference between two consecutive iterations is negligible until around 10 dB before their very close saturating instants. The size of the cells matter here. In small sized cells, it is possible to have high SNR conditions. This is especially a particular situation in pico and microcells where HSDPA service will be mostly given. In that case, going to a high number of iterations might pay off. In large cells like macro or rural ones, however, noise will become comparable to interference. Then limiting the iterations to 1, or using only the equalizer (i.e iteration 0) or even a Rake replacement would be better since each iteration would then amplify the noise and deteriorate the performance instead of improving it. When we observe the highest iteration curve, we see that before saturation it follows a straight line. Although not verified yet, when we carry the iterations to large numbers we expect the slope of the final plot to overlap with that of symbol level LMMSE.

We now elaborate on the results in Fig. 14 again from the receiver in Fig. 10, this time hard subtracting the pilot tones from both BSs and introducing hyperbolic tangent and hard decision functionalities over the HSDSCH codes in the own cell. By first comparing the linear estimates with the linear estimates obtained previously in Fig. 13 we can say that there is very little improvement from pilot tone cancellation. As seen in Fig. 14, we didn't obtain any difference between the performances of hyperbolic tangent and hard decisions either; so we conclude that hard decisions are preferable due to their simplicity. Compared to the linear treatment, however, both perform much better. Furthermore, the gap opens with every iteration. That is to say, for example, the difference at high SNR regions between s_4 or m_4 to c_4 (10 dB) is much higher than the difference between s_1 or m_1 to c_1 (1 dB). High SNR conditions being a more probable deployment scenario, HSDPA will then highly benefit from an high order receiver with proposed nonlinearities. Because, as we mentioned before, unlike for dedicated channels (DCHs) where it serves only for the benefit of the base station, for HSDSCHs, a mobile terminal directly benefits from having an advanced receiver by obtaining more data rate once the connection is established and by increasing the chance of getting a connection if fairness is partially sacrificed for capacity in user scheduling.

VII. CONCLUSIONS

In this paper we derived iterative receivers from polynomial expansion. We stressed the importance of the choice of linear filters and the feedback functionalities for guaranteeing a fast convergence under

realistically high loading factors. We also briefly discussed the relation between the expansion order required and the input E_b/N_0 . We concluded that this type of receivers constitutes a perfect candidate for HSDPA type services.

Some issues have not yet been covered in this paper such as the degradation of performance under channel estimation errors and the influence of fixed point implementation inaccuracies. These are topics for further investigation.

REFERENCES

- [1] R. Price and P. E. Green, "A communication technique for multipath channels," *Proc. of the IRE*, vol. 46, pp. 555–570, March 1958.
- [2] A. Klein, "Data detection algorithms specially designed for the downlink of CDMA mobile radio systems," in *Proc. VTC*, Phoenix, AZ, May 1997, pp. 203–207.
- [3] I. Ghauri and D. T. M. Slock, "Linear receivers for the DS-CDMA downlink exploiting orthogonality of spreading sequences," in *Proc. 32nd Asilomar Conf. on Signals, Systems & Computers*, Pacific Grove, CA, November 1998.
- [4] C. D. Frank and E. Visotsky, "Adaptive interference suppression for direct-sequence CDMA systems with long spreading codes," in *Proc. 36th Annual Allerton Conference on Communication, Control, and Computing*, Urbana-Champaign, IL, September 1998.
- [5] T. P. Krauss, M. D. Zoltowski, and G. Leus, "Simple MMSE Equalizers for CDMA Downlink to Restore Chip Sequence: Comparison to Zero-Forcing and RAKE," in *Proc. ICASSP 2000*, October 2000.
- [6] S. Moshavi, "Multi-user detection for DS-CDMA communications," *IEEE Communications Magazine*, pp. 124–136, October 1996.
- [7] S. Verdú, *Multuser Detection*. Cambridge University Press, 1998.
- [8] R. Lupas and S. Verdú, "Linear multiuser detectors for synchronous code-division multiple-access channels," *IEEE Transactions on Information Theory*, Vol.IT-35,pp. 123-136, Jan 1989.
- [9] U. Madhow and M. Honig, "Mmse interference suppression for direct-sequence spread-spectrum cdma," *IEEE Transactions on Communications Theory*, Vol.42,pp. 3178-3188, Dec 1994.
- [10] D. Divsalar, M. Simon, and D. Raphaeli, "Improved parallel interference cancellation," *IEEE Transactions on Communications Theory*, Vol.46,pp. 258-268, Feb 1998.
- [11] M. Varanasi and B. Aazhang, "Multistage detection in asynchronous code-division multiple-access communications," *IEEE Transactions on Communications*, vol. 38, no. 4, pp. 509–519, April 1990.
- [12] R. M. Buehrer, S. P. Nicoloso, and S. Gollamudi, "Linear versus nonlinear interference cancellation," *Journal of Communications and Networks*, vol.1, June 1999.
- [13] N. Mehta, L. Greenstein, T. Willis, and Z. Kostic, "Analysis and results for the orthogonality factor in wcdma downlinks," *Proc. Vehicular Technology Conference*, May 2002.
- [14] K. Pedersen and P. Mogensen, "The downlink orthogonality factors influence on wcdma system performance," *Proc. Vehicular Technology Conference*, September 2002.
- [15] S. Moshavi, E. Kanterakis, and D. L. Schilling, "Multistage linear receivers for ds-cdma systems," *International Journal of Wireless Information Networks*, Vol.3, No.1, 1996.
- [16] M. Madcour, S. Gupta, and Y. Wang, "Successive interference cancellation algorithms for downlink w-cdma communications," *IEEE Transactions on Wireless Communications*, vol.1, No.1, Jan 2002.
- [17] R. Irmer, A. Nahler, and G. Fettweis, "On the impact of soft decision functions on the performance of multistage parallel interference cancelers for cdma systems," *Proc. VTC Spring 2001, Rhodes, Greece*, May 2001.

- [18] "3GPP TS 25.848, Physical Layer Aspects of HSDPA, [Online]. Available:<http://www.3gpp.org/ftp/Specs>."
- [19] "3GPP TS 25.855, UTRA High Speed Downlink Packet Access; Overall UTRAN description, [Online]. Available: <http://www.3gpp.org/ftp/Specs>."
- [20] J. Sadowsky, D. Yellin, S. Moshavi, and Y. Perets, "Cancellation accuracy in cdma pilot interference cancellation," *Proc. Vehicular Technology Conf.*, April 2003.
- [21] I. Ghauri and D. T. M. Slock, "Mmse-zf receiver and blind adaptation for multirate cdma," in *Proc. VTC'99*, Sept 1999.
- [22] C. Papadias and D. Slock, "Fractionally spaced equalization of linear polyphase channels and related blind techniques based on multichannel linear prediction," *IEEE Transactions on Signal Processing*, Vol.47, No.3, March 1999.
- [23] G. Bottomley, T. Ottoson, and Y. Wang, "A generalized rake receiver for interference suppression," *IEEE Journal Selected Areas Communications*, vol. 18, pp. 1536–1545, August 2000.

Ahmet Baştuğ was born in Kütahya, Turkey in 1976. He received the B.Sc. degree with high honors from Middle East Technical University (METU), Ankara in 1999 and the M.Sc. degree from Boğaziçi University, Istanbul in 2002, both in electrical engineering. For his undergraduate education he was awarded a full scholarship by METU (and also a not-used one by the Turkish Ministry of Education for American universities) due to his high rank among university applicants. From 1998 to 1999 he was with Karel Electronics, Ankara as an FPGA design engineer and from 1999 to 2002 with ST-Microelectronics, Istanbul (formerly Alcatel Microelectronics) as an ASIC design engineer where he participated in the designs of IEEE 802.11a & HIPERLAN-2 Wireless-LAN and ADSL/VDSL modem chip sets. In November 2002, he joined Eurecom Institute, France as a phd candidate of E.N.S.T. Paris. Since March 2004, he is with Philips Semiconductors as a UMTS algorithm development engineer. He is conducting his phd study with Prof. Slock within the scope of physical layer receivers and channel estimation for UMTS mobile terminals, concentrating particularly on HSDPA. He is the recipient of the IEEE-SIU2004 student best paper award.

Dirk T.M. Slock received the engineering degree from the University of Gent, Belgium, in 1982. In 1984 he was awarded a Fulbright scholarship to Stanford University, Stanford, CA, from which he received the M.S. degree in electrical engineering, the M.S. degree in statistics, and the Ph.D. degree in electrical engineering in 1986, 1989, and 1989, respectively. While at Stanford, he developed new fast recursive least-squares (RLS) algorithms for adaptive filtering. From 1989 to 1991, he was a member of the research staff at the Philips Research Laboratory, Gent. In 1991, he joined the Eurecom Institute, Sophia Antipolis, France, where he is now Professor. At Eurecom, he teaches statistical signal processing and speech coding for mobile communications. His research interests include DSP for mobile communications [antenna arrays for (semi-blind) equalization/interference cancellation and spatial division multiple access, space-time processing and coding, and channel estimation] and adaptation techniques for audio processing. More recently, he has focused on receiver design, downlink antenna array processing, and source coding for third-generation systems and introducing spatial multiplexing in existing wireless systems. In 2000, he cofounded SigTone, a start-up developing music signal processing products. He is also active as a consultant on xDSL and DVB-T systems. Dr. Slock received one best journal paper award from the IEEE-SP and one from EURASIP in 1992. He received two IEEE-Globecom98 best student paper awards. He was an associate editor for the IEEE TRANSACTIONS ON SIGNAL PROCESSING from 1994 to 1996. He was an associate editor for the IEEE-SP Transactions in 1994-96. He is an associate editor for the EURASIP Journal on Applied Signal Processing (JASP) and a guest editor for three special issues in JASP. He has been a member of IEEE-SP Technical Committees for over ten years, lately on DSP for Communications.

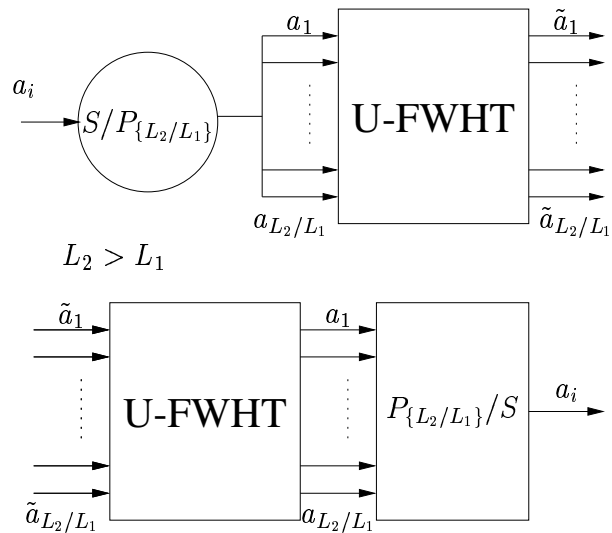


Fig. 1. Transformations between actual and pseudo symbols

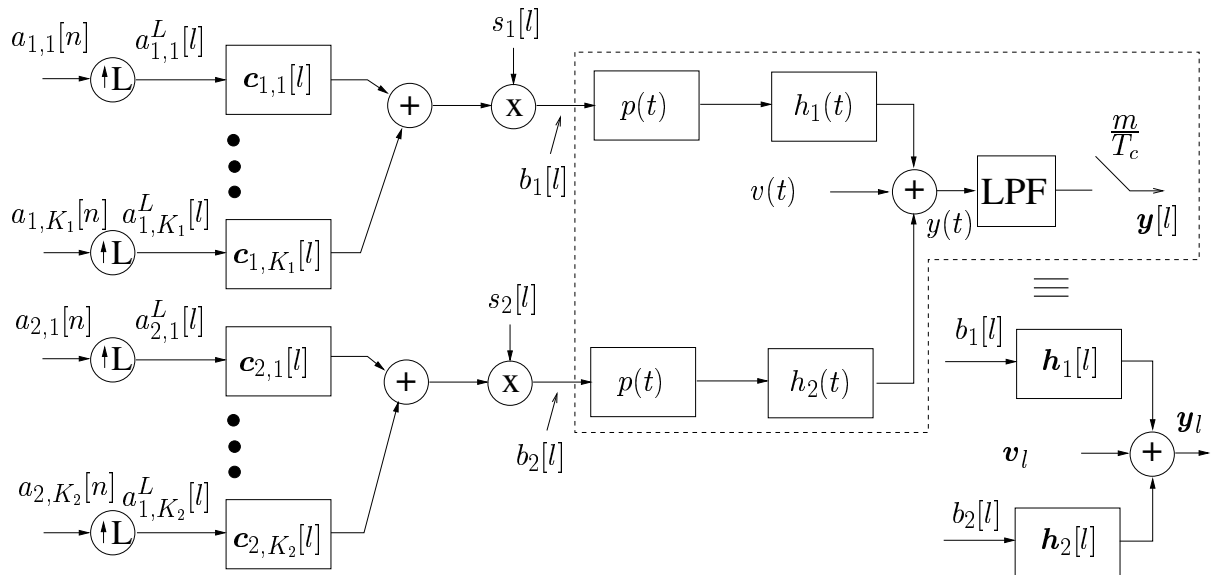


Fig. 2. Baseband downlink transmission model

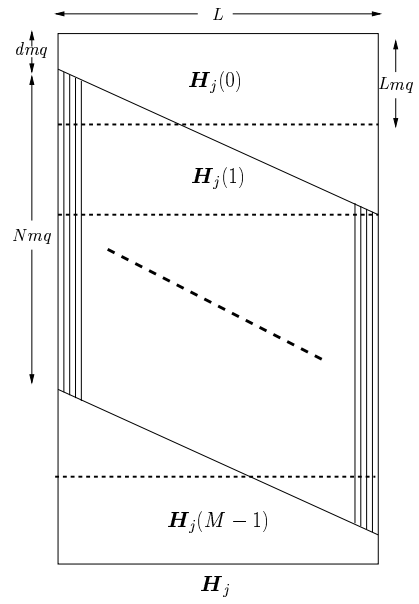


Fig. 3. Channel impulse response of $\mathbf{H}_j(z)$.

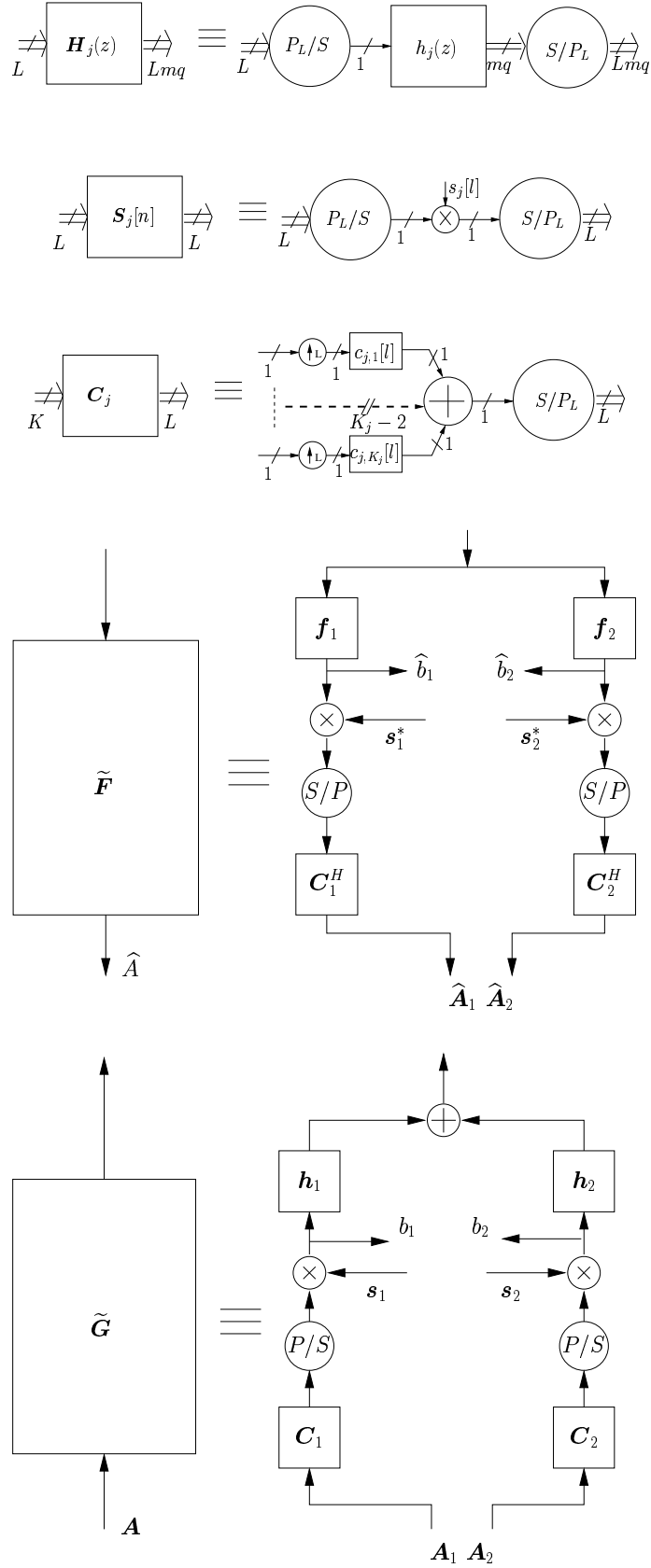


Fig. 4. Symbol rate and chip rate equivalent representations

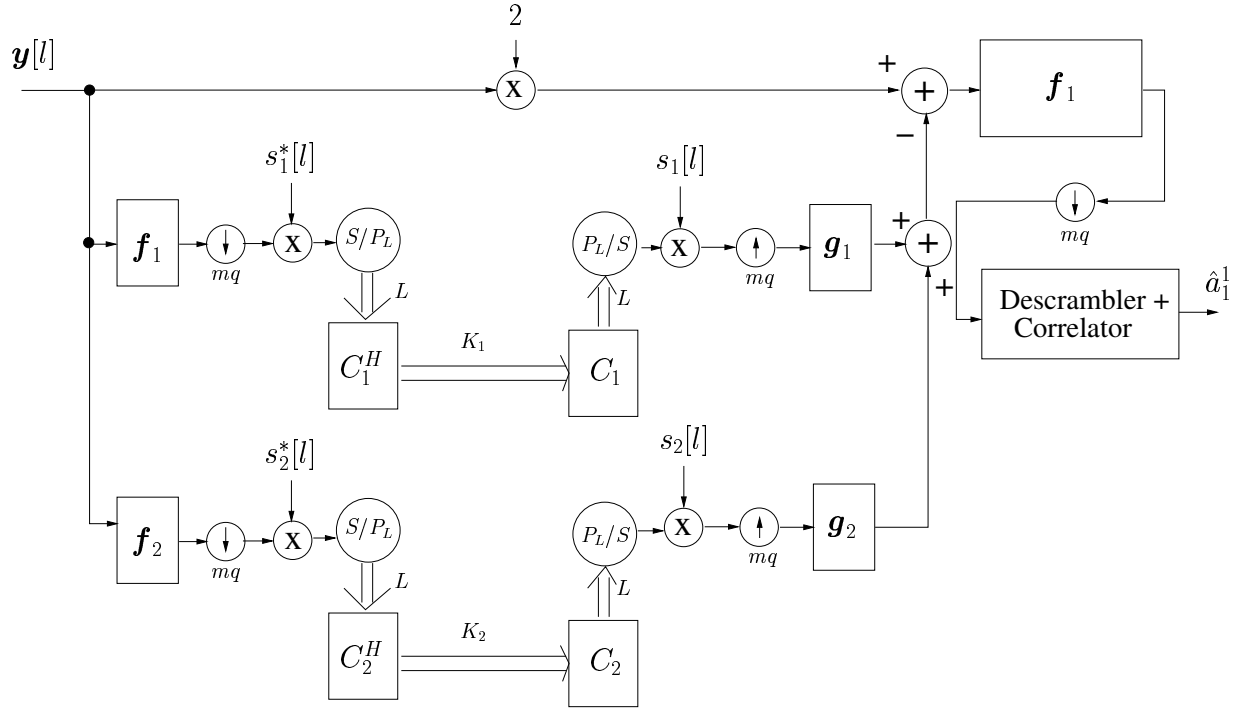


Fig. 5. Chip rate first order polynomial expansion structure.

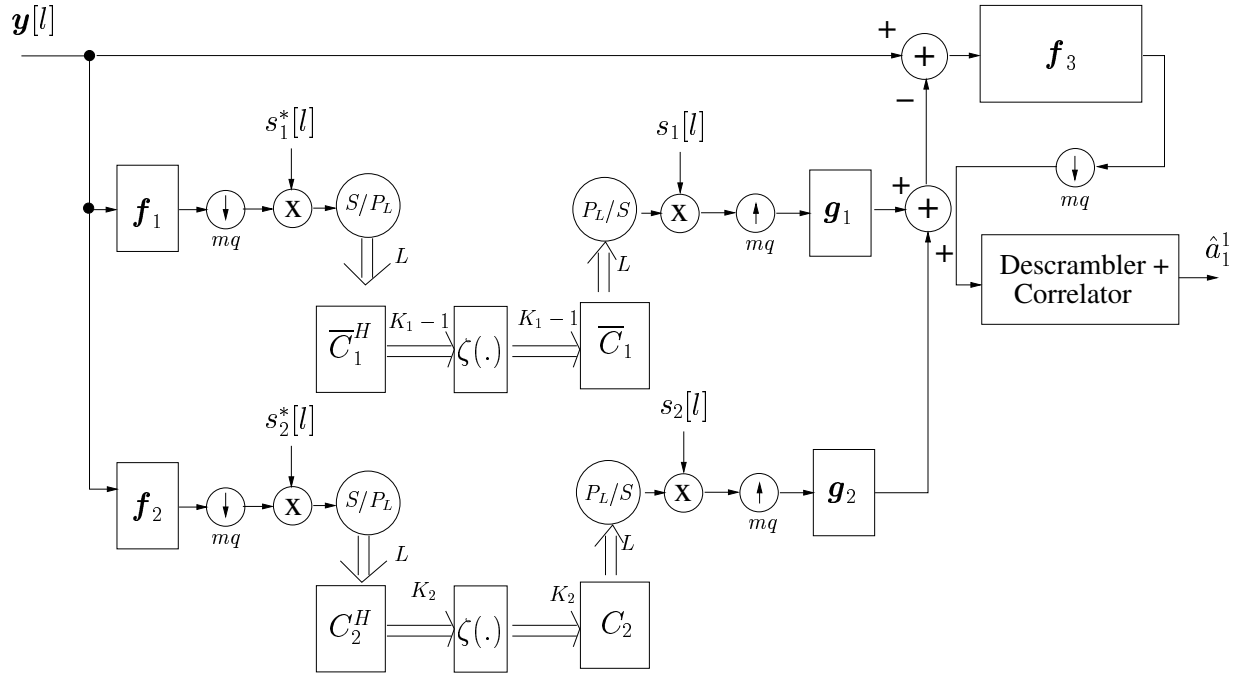


Fig. 6. Chip rate first order interference canceller structure

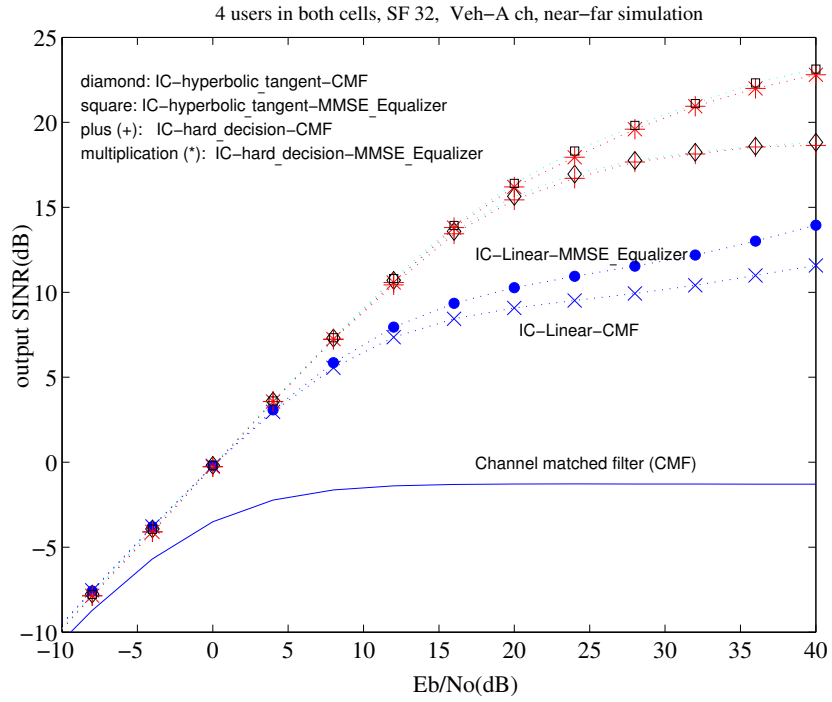


Fig. 7. Output SINR vs input Eb/No, 12.5% loaded BSs, near-far situation

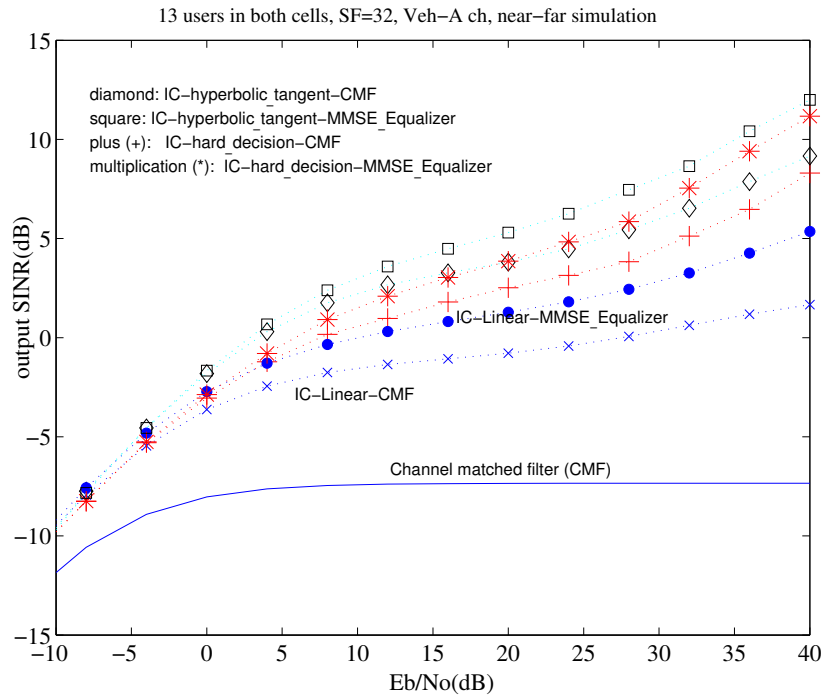


Fig. 8. Output SINR vs input Eb/No, 40% loaded BSs, near-far situation

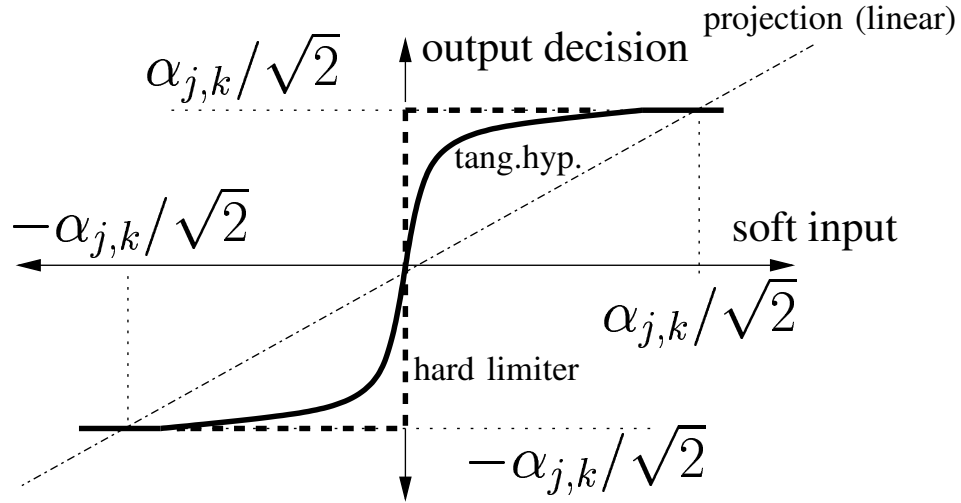


Fig. 9. Linear, tangent hyperbolic and hard limiter decisions for real/imaginary parts of QPSK symbols

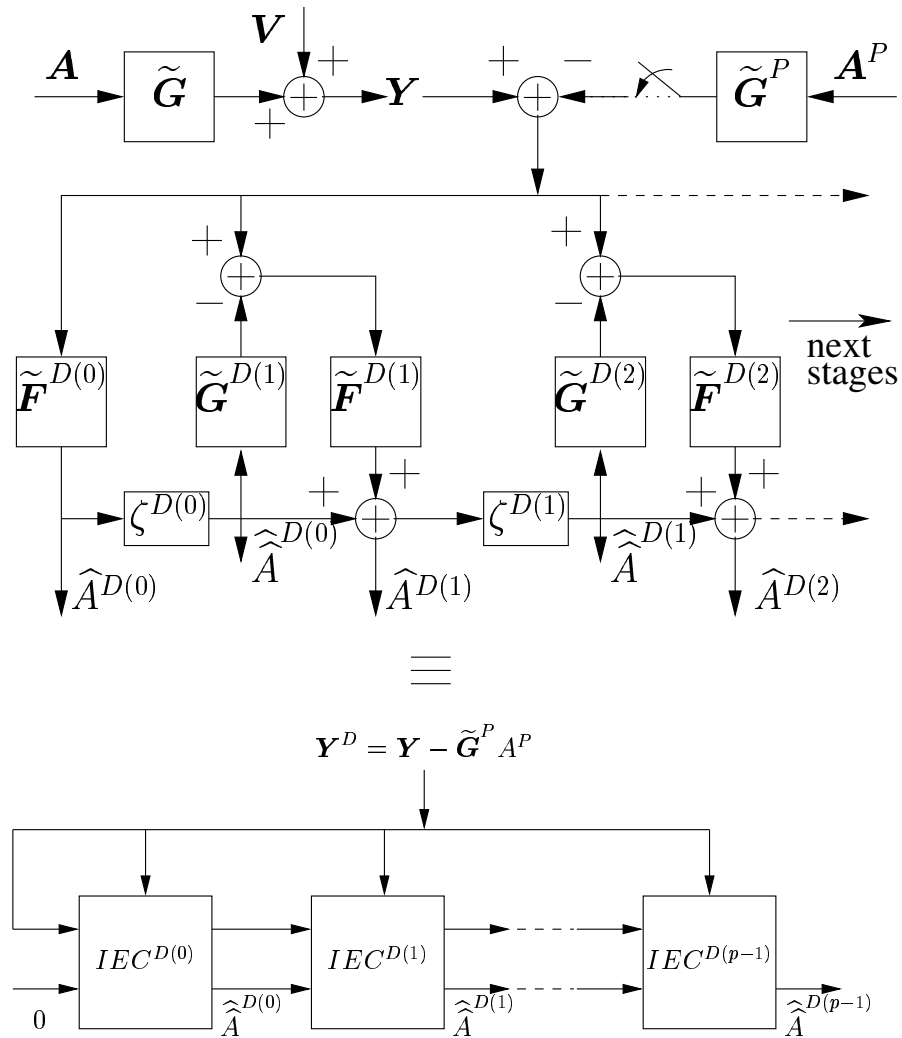


Fig. 10. Polynomial expansion receiver

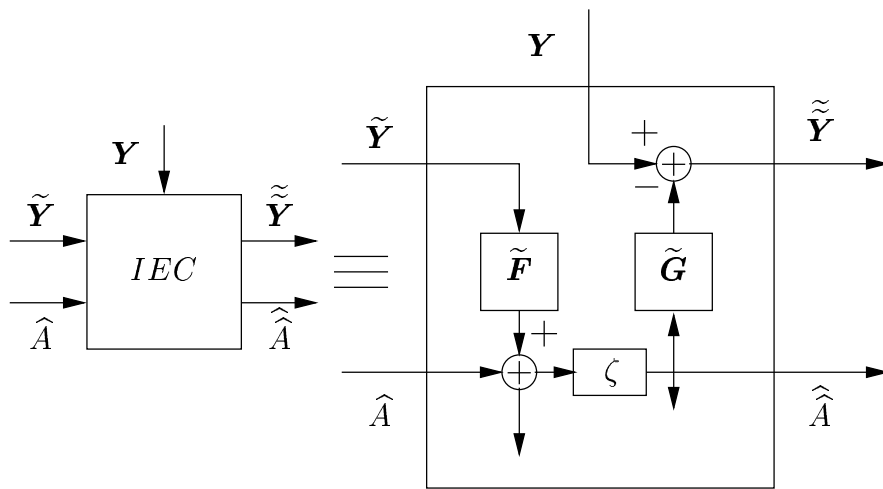


Fig. 11. Interference estimator and canceller block

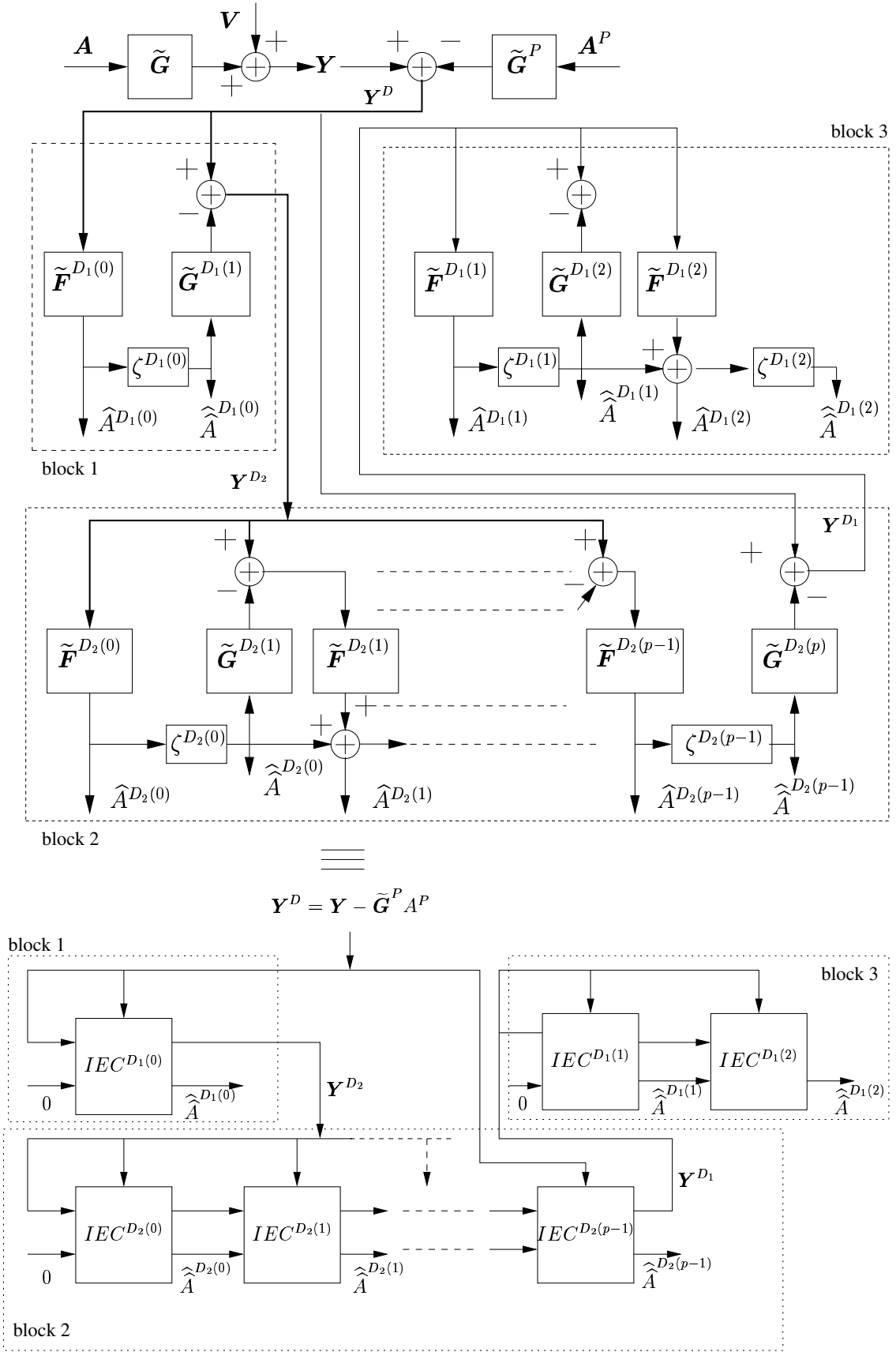


Fig. 12. Hybrid polynomial expansion receiver

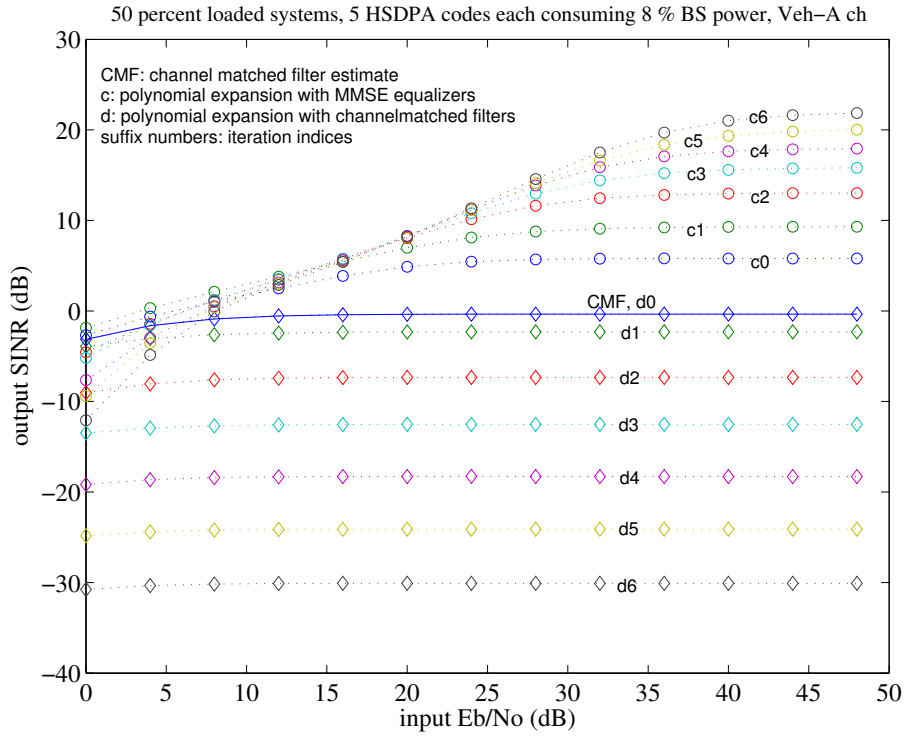


Fig. 13. Polynomial expansion with {channel matched filters, MMSE equalizers}

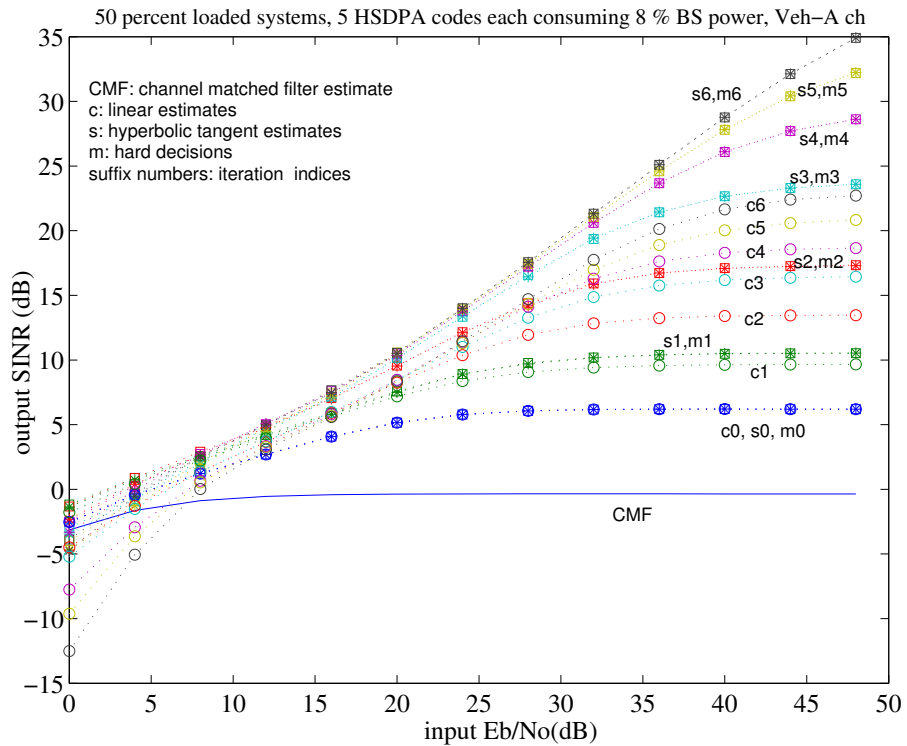


Fig. 14. Polynomial expansion with MMSE equalizers and {linear, hyperbolic tangent, hard} decisions